

## Experimental Electron Density Study of Tetrakis- $\mu$ -(acetylsalicylate)dicopper(II): a Polymeric Structure with Cu $\cdots$ Cu Short Contacts

Nouzha Bouhaida,<sup>†</sup> Miguel A. Méndez-Rojas,<sup>\*‡</sup> Aarón Pérez-Benítez,<sup>§</sup> Gabriel Merino,<sup>||</sup> Bernard Fraisse,<sup>⊥</sup> and Nour Eddine Ghermani<sup>\*⊥,⊗</sup>

<sup>†</sup>Laboratoire des Sciences des Matériaux (LSM), Université Cadi Ayyad, Faculté des Sciences Semlalia, Boulevard Prince Moulay Abdallah, BP 2390, 40000 Marrakech, Morocco, <sup>‡</sup>Departamento de Ciencias Químico-Biológicas, Universidad de las Américas-Puebla, Ex-Hacienda de Sta. Catarina Mártir, A.P. 100, Cholula 72820, Puebla, Puebla, México, <sup>§</sup>Facultad de Ciencias Químicas, Benemérita Universidad Autónoma de Puebla, Puebla, Puebla, México, <sup>||</sup>Facultad de Química, Universidad de Guanajuato, Guanajuato, México, <sup>⊥</sup>Laboratoire Structures, Propriétés et Modélisation des Solides (SPMS) UMR CNRS 8580, Ecole Centrale Paris, 1, Grande Voie des Vignes, 92295 Châtenay-Malabry, France, and <sup>⊗</sup>Laboratoire de Physique Pharmaceutique UMR CNRS 8612, Université Paris Sud 11, Faculté de Pharmacie, 5, Rue Jean-Baptiste Clément, 92296 Châtenay-Malabry, France

Received January 15, 2010

The electron density, its topological features, and the electrostatic potential of tetrakis- $\mu$ -(acetylsalicylate)dicopper(II), Cu[C<sub>9</sub>H<sub>7</sub>O<sub>4</sub>]<sub>2</sub>, have been derived from an accurate high-resolution diffraction experiment at 100 K. This complex exhibits a polymeric structure involving one acetyl oxygen atom as a bridge in the solid state. Only van der Waals interactions between the polymeric chains are observed. The copper cation is octahedrally coordinated with five oxygen atoms of the aspirinate ligands and one adjacent Cu with short Cu  $\cdots$  Cu contact distances in the range of 2.6054(1) Å. The Cu–O bond lengths are equal to 1.96 Å except the apical one which is 2.2183(7) Å. The multipole refinements were carried out using the Hansen–Coppens model coded in the MOPRO computer program. Starting from the 3d<sup>10</sup>4s<sup>1</sup> copper electron configuration, the electron density analysis and Cu d-orbital populations reveal that the observed configuration is close to being [Ar]3d<sup>9</sup>4s<sup>1</sup>. As expected from the ligand field theory, the most depopulated 3d-orbital is the d<sub>x<sup>2</sup>-y<sup>2</sup></sub> (1.17 e) one with lobes pointing toward the carboxylic oxygen atoms. Conversely, the d<sub>z<sup>2</sup></sub> is the most populated orbital for a z-axis directed along the Cu  $\cdots$  Cu bond. The atomic charges were derived from a  $\kappa$ -refinement and yielded a metal net charge of +1.20(3) e. Deficits of +0.72(6) and +0.59(7) e are obtained for the acetyl carbon atoms of the aspirinate ligands, those involved in the drug activity of aspirin. Comparisons are made to the results of our previous work on the zinc-aspirinate complex.

### 1. Introduction

The electron density distribution in molecules and chemical systems is essential to understand and explain the properties of several materials of pharmaceutical importance. High resolution X-ray crystallography has become a powerful tool to deeply investigate electron density in different kinds of crystalline materials.<sup>1</sup> During the past decade, considerable improvements of bright light sources, detectors, experimental setups, and methodology developments make charge density study results more accurate and further the frontiers of knowledge of even elusive chemical bonding.<sup>2</sup> Among the wide

variety of existing compounds, transition metal complexes are particularly investigated because of their great importance in fundamental and applied chemistry, biochemistry, and pharmacology. In the life sciences and in biology in particular, metals like copper, zinc, or iron play a crucial role in metabolic functionalities of living organisms. Sometimes, excess or deficiency of a particular metal increases the risk of lethal pathologies or poisoning. By mimicking the biological mechanisms, the pharmaceutical researchers try to improve the drug activity by associating organic molecules with metals. This can improve metal/drug transportation across biological membranes yielding a possible enhancement of drug activity or an overcoming of metal deficiency. Non-steroidal anti-inflammatory (NSAI) agents like aspirin (acetylsalicylic acid, hereafter Asp) are among the most used drugs throughout the world. However, depending on the administered dose, these drugs are well-known to exhibit side effects like gastrointestinal complications especially for aged patients. To reduce the dose of the drug and

\*To whom correspondence should be addressed. E-mail: noureddine.ghermani@u-psud.fr. Phone: +33(0)14683 56 48. Fax: +33(0)146 83 58 82. E-mail: miguela.mendez@udlap.mx. Phone: +52(222) 229 2607. Fax: +52(222) 229 2416.

(1) Coppens, P. In *X-ray Charge Densities and Chemical Bonding*; IUCr, Oxford University Press: New York, 1997.

(2) Koritsanszky, T. S.; Coppens, P. *Chem. Rev.* **2001**, *101*, 1583.

its toxicity, one option is to associate aspirin with metals such as Cu, Fe, Zn, or Mn. The scientific literature is rich in studies dedicated to the comparison of biological activity of the parent and metal-based drugs.<sup>3,4</sup>

Some years ago, we reported the electron density and electrostatic properties of the zinc-aspirinate complex  $\text{Zn}(\text{Asp})_2(\text{H}_2\text{O})_2$ .<sup>5</sup> In that case, the zinc cation has a tetrahedral coordination and is bonded to two deprotonated aspirin molecules and two water molecules. The aspirinate anion acts as a monodentate ligand involving one oxygen atom of the carboxylate group  $\text{COO}^-$ . It was shown in the previous study that the 3d valence orbital of Zn remains unperturbed and only the 4s orbital is engaged in the interaction with the organic ligands. All attempts to refine the 3d orbital electron population were unsuccessful. It was concluded that the tetrahedral coordination of zinc in  $\text{Zn}(\text{Asp})_2(\text{H}_2\text{O})_2$  does not facilitate the interaction of the 3d orbital with the ligands. A more favorable situation involving the 3d orbital is found for the copper-aspirinate which is the subject of the present study. The Cu cation is octahedrally coordinated, and the studied complex exhibits a  $\text{Cu}\cdots\text{Cu}$  distance of 2.6045(1) Å. It is important to mention that metal complexes with the general formula  $\text{Cu}_2(\text{OOCR})_4(\text{L})_2$  have been known for almost 60 years, and that their structures and magnetic properties have been widely studied (they possess a singlet ground state with a low lying triplet excited state). From more than 300 crystal structures reported in the Cambridge Structural Database (CSD), around 10% possess  $\text{Cu}\cdots\text{Cu}$  distances as short or shorter than 2.6045(1) Å (as reported in this work), with an average value of 2.634 Å. Very small crystals have been used in the first crystallographic study of tetrakis- $\mu$ -(acetylsalicylate)dicationic copper(II) complex.<sup>6,7</sup> Suitable crystal samples for charge density studies were recently obtained by an improved electro-synthesis experiment.<sup>8,9</sup> High resolution X-ray diffraction data collected at 100 K were used to refine the electron density for the tetrakis- $\mu$ -(acetylsalicylate)dicationic copper(II) complex. Previously, the electron density refinement of the zinc-aspirinate complex<sup>5</sup> has been carried out using the MOLLY program based on the multipole electron Hansen–Coppens model.<sup>10</sup> The new MOPRO and VMOPRO computer programs based on the same density model were here used for the refinement of the electron density of tetrakis- $\mu$ -(acetylsalicylate)dicationic copper(II) complex and for the determination of the electrostatic properties.<sup>11,12</sup> The topological features of the electron density and electrostatic potential are presented here.

## Materials and Methods

**Synthesis and Crystallization.** Single crystals with the largest dimensions ranging from 0.3 to 0.8 mm, very suitable for X-ray

analysis, were obtained by direct electro-synthesis with in situ generation of supporting electrolyte.<sup>8</sup> In summary, a copper anode was electrochemically dissolved in an aqueous solution containing a known amount of acetylsalicylic acid (aspirin) at room temperature, using a Pt electrode as cathode and a saturated calomel electrode (SCE) as reference electrode. A constant voltage of 6 V was imposed for a period of 360 min. After that time, the mixture was let stand at ambient conditions to complete further acid/base reactions. Forty eight hours later, good quality, large hexagonal prismatic blue single crystals of tetrakis- $\mu$ -(acetylsalicylate)dicationic copper(II) were obtained. Details on the synthetic procedure have been previously reported.<sup>9</sup>

**Data Collection.** A suitable crystal sample of a tetrakis- $\mu$ -(acetylsalicylate)dicationic copper(II) blue crystal with dimensions  $0.30 \times 0.25 \times 0.20$  mm was used for the high resolution X-ray diffraction experiment. The data were collected at 100.0(1) K on a Bruker-SMART three axis diffractometer equipped with a SMART 1000 CCD area detector using graphite monochromated Mo  $K\alpha$  X-radiation (wavelength  $\lambda = 0.71073$  Å). The area detector surface was placed at 5 cm from the crystal sample. The diffraction data were collected at six different detector positions:  $2\theta = 0, \pm 25, \pm 70, 80^\circ$  where  $\theta$  is the Bragg angle. The data spots were recorded as  $\omega$ -scans ( $\Delta\omega = 0.15^\circ$ ) to reconstruct accurate three-dimensional diffracted intensity profiles. According to the  $\theta$ -dependence of the diffracted intensities, the chosen exposure times were 10, 25, 40, and 45 s for the detector positions at  $2\theta = 0, \pm 25, \pm 70, 80^\circ$ , respectively. The maximum resolution reached for this experimental data set is  $(\sin \theta/\lambda)_{\text{max}} = H/2 = 1.106 \text{ \AA}^{-1}$ , where  $H$  is the Bragg vector modulus. A total of 143962 symmetry-equivalent and redundant measurements were collected in this experiment. The Lorentz-polarization correction and the integration of the diffracted intensities were performed with the SAINT software package.<sup>13</sup> An empirical absorption correction was applied using the SADABS<sup>13</sup> computer program. The SORTAV<sup>14</sup> program was used for sorting and averaging data in the  $2/m$  point group giving a total of 17882 unique reflections and a final internal factor  $R_{\text{int}} = 0.0303$ . Details of the X-ray diffraction experiment conditions and the crystallographic data for the tetrakis- $\mu$ -(acetylsalicylate)dicationic copper(II) complex are given in Table 1.

**Electron Density Refinements.** In the Hansen–Coppens model<sup>10</sup> that we have used the molecular electron density is the sum of pseudoatomic contributions expressed as

$$\rho_{\text{at}}(\underline{r}) = \rho_{\text{core}}(\underline{r}) + P_{\text{val}}\kappa^3\rho_{\text{val}}(\kappa\underline{r}) + \sum_{l=0}^{l_{\text{max}}} \kappa^{l^3} R_{nl}(\kappa'\underline{r}) \sum_{m=0}^l P_{lm\pm} y_{lm\pm}(\theta, \varphi) \quad (1)$$

where  $\rho_{\text{core}}(r)$ ,  $\rho_{\text{val}}(r)$  describe the frozen core and valence spherical densities both obtained from the Hartree–Fock wave functions of the free atoms or ions.<sup>15</sup>  $\kappa$  is a contraction–expansion coefficient of the spherical valence electron density and  $P_{\text{val}}$ , the corresponding refined electron population. Therefore, the atomic charge can be estimated as  $q = P_{\text{val}} - N_{\text{val}}$  where  $N_{\text{val}}$  is the valence population of the free atom or ion. The aspherical part of the pseudoatom electron density is projected onto a real normalized harmonics  $y_{lm\pm}$  basis set ( $l = 0$  (monopole) to 4 (hexadecapole)) and modulated by a Slater-type radial function  $R_n(r) = Nr^{2l} \exp(-\xi r)$ , where  $N$  is the normalization factor. In eq 1,  $\kappa'$  is a contraction–expansion coefficient used to adjust the maximum

- (3) Cameron, B. R.; Baird, I. R. *J. Inorg. Biochem.* **2001**, *83*(2–3), 233.  
 (4) Sorenson, J. R. J. In *Handbook of Metal-Ligand Interactions in Biological Fluids: Bioinorganic Medicine*; Berthon, G.; Ed.; M. Dekker: New York, 1995; Vol. 2.  
 (5) Spasojević-de Biré, A.; Bouhaida, N.; Kremenović, A.; Morgant, G.; Ghermani, N. E. *J. Phys. Chem.* **2002**, *106*(50), 12170.  
 (6) Manojlović-Muir, L. *Chem. Commun.* **1967**, 1057.  
 (7) Manojlović-Muir, L. *Acta Crystallogr.* **1973**, *B29*, 2033.  
 (8) Méndez-Rojas, M. A.; Córdova-Lozano, F.; Gojon-Zorrilla, G.; González-Vergara, E.; Quiroz, M. A. *Polyhedron* **1999**, *18*, 2651.  
 (9) García, F.; Méndez-Rojas, M. A.; González-Vergara, E.; Bernès, S.; Quiroz, M. A. *Acta Crystallogr.* **2003**, *E59*, m1171.  
 (10) Hansen, N. K.; Coppens, P. *Acta Crystallogr.* **1978**, *A34*, 909.  
 (11) Guillot, B.; Viry, L.; Guillot, R.; Lecomte, C.; Jelsch, C. *J. Appl. Crystallogr.* **2001**, *34*, 214.  
 (12) Jelsch, C.; Guillot, B.; Lagoutte, A.; Lecomte, C. *J. Appl. Crystallogr.* **2005**, *38*, 38.

(13) *ASTRO (5.007)*, *SAINTE (5.007)*, and *SADABS (5.007)*; *Data Collection and Processing Software for the SMART System (5.054)*; Siemens (BRUKER-AXS) Analytical X-ray Instruments Inc.; Madison, WI, 1998.

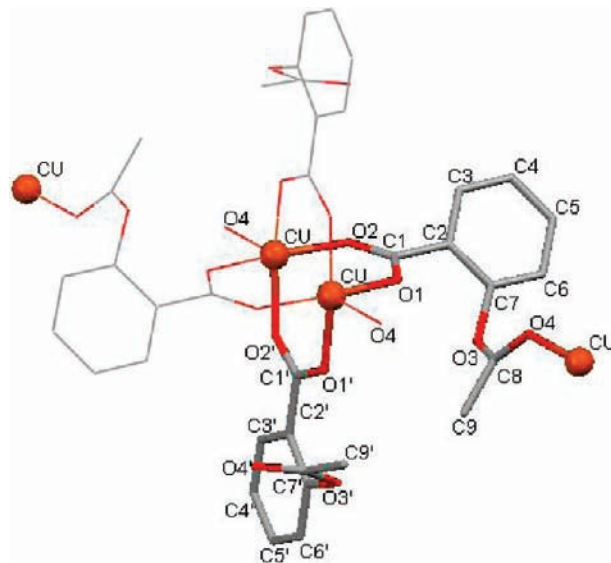
(14) Blessing, R. H. *J. Appl. Crystallogr.* **1997**, *30*, 421.

(15) Clementi, E.; Roetti, C. *Atomic data and Nuclear data tables*; Academic Press: New York, 1974; Vol. 14, p 177.

**Table 1.** Experimental and Refinement Details for Tetrakis- $\mu$ -(acetylsalicylate)-dicopper(II) Complex

empirical formula	[Cu(C <sub>9</sub> H <sub>7</sub> O <sub>4</sub> ) <sub>2</sub> ]
formula weight	421.9
temperature	100.0(1) K
wavelength	0.71073 Å
crystal system	monoclinic
space group	<i>P</i> 2 <sub>1</sub> / <i>n</i>
unit cell dimensions	<i>a</i> = 8.1606(3) Å <i>b</i> = 10.3474(4) Å <i>c</i> = 20.7708(5) Å $\beta$ = 98.152(1)°
volume	1736.18(3) Å <sup>3</sup>
<i>Z</i>	4
density (calculated)	1.610 Mg/m <sup>3</sup>
absorption coefficient	1.303 mm <sup>-1</sup>
<i>F</i> (000)	860
crystal size	0.30 × 0.25 × 0.20 mm <sup>3</sup>
$\theta$ range for data collection	1.99 to 51.88°
[(sin $\theta$ )/ $\lambda$ ] <sub>max</sub>	1.106 Å <sup>-1</sup>
index ranges	-17 ≤ <i>h</i> ≤ 17 -22 ≤ <i>k</i> ≤ 22 -44 ≤ <i>l</i> ≤ 44
reflections collected	143962
independent reflections	17882 [ <i>R</i> <sub>int</sub> = 0.0303]
completeness to $\theta$ = 51.88°	95.4% (100% completeness up to 0.91 Å <sup>-1</sup> )
spherical refinement method	full-matrix least-squares on <i>F</i> <sup>2</sup>
data/restraints/parameters	17685/0/300
goodness-of-fit on <i>F</i> <sup>2</sup>	0.879
<i>R</i> indices (all data)	<i>R</i> 1 = 0.0365, <i>wR</i> 2 = 0.0572
final <i>R</i> indices [ <i>I</i> > 2 $\sigma$ ( <i>I</i> )]	<i>R</i> 1 = 0.0253
largest diff. peak and hole	0.750 and -0.770 e Å <sup>-3</sup>
multipolar refinement method	full-matrix least-squares on <i>F</i>
data [ <i>I</i> > 3 $\sigma$ ( <i>I</i> )]	12633
goodness-of-fit on <i>F</i>	0.727
final <i>R</i> indices	<i>RF</i> = 0.0173, <i>wRF</i> = 0.0157 <i>RF</i> <sup>2</sup> = 0.0220, <i>wRF</i> <sup>2</sup> = 0.0309

of the radial function and  $P_{lm\pm}$  are the multipole populations of the pseudoatom electron deformation density. The exponents<sup>16</sup>  $\xi_l$  (in bohr<sup>-1</sup>) of the radial functions are chosen equal to 3.1, 4.5, and  $n_l = 2, 2, 3$  up to octupoles ( $l = 3$ ) for C and O atoms respectively;  $\xi_l = 2.00$  bohr<sup>-1</sup> and  $n_l = 1$  (dipole level,  $l = 1$ ) for the hydrogen atoms. For the copper atom having an electronic configuration 3d<sup>10</sup>4s<sup>1</sup>, only the 3d population was refined as a  $P_{val}$  parameter (eq 1). The copper monopole  $P_{00}$  was kept fixed to 1.0 corresponding to the population of the 4s orbital; the refinement of this parameter yields unrealistic results. It also holds true for all attempts to hybridize 3d and 4s orbitals. This refinement strategy is different from that used in the previous study of zinc-aspirinate complex where only the 4s population was refined using the MOLLY program.<sup>5,10</sup> MOPRO program<sup>11,12</sup> of the electron density refinement combines both conventional and conjugate gradient least-squares procedures and the correlations between parameters are better controlled than in MOLLY. The deformation density revealing the 3d orbital lobes is here described using the even orders  $l = 0, 2, 4$  of the multipolar expansion given in the previous equation. The  $\xi_l$  exponents of the radial function for Cu are all chosen equal to 8.8 bohr<sup>-1</sup> and  $n_l = 4, 4, 4, 4$  up to hexadecapole level ( $l = 4$ ). The crystal structure of the copper-aspirinate is shown in Figure 1. To make comparisons with the Zn-aspirinate compound,<sup>5</sup> the same numbering scheme was used in this study. For the multipole refinement, the local frame axes for Cu were chosen as conventional: *z*-axis is along the Cu...Cu contact and *x*-axis is directed toward oxygen O1. In the first cycles of refinements, valence and multipole populations and  $\kappa$ 's were constrained to be the same for the chemically equivalent atoms. These constraints were relaxed at the end of the refinement except some carbon and hydrogen atoms of the phenolic rings and methyl groups: C3=C4=C5=C6, H3=H4=H5=H6,

**Figure 1.** Structure and numbering scheme of the tetrakis- $\mu$ -(acetylsalicylate)dicopper(II) complex. Copper atoms are represented as spheres and the two aspirinate ligands of the asymmetric unit capped sticks. Hydrogen atoms are omitted for clarity.

and H91=H92=H93 for both primed and unprimed ligands (see Figure 1). After the multipole refinement, the atomic charges of the title compound were estimated from a  $\kappa$ -refinement using only  $P_{val}$  and  $\kappa$  of eq 1.

**Deformation Density Maps and Topological Analysis.** The VMOPRO<sup>11,12</sup> computer program was used to map out the static electron deformation density maps and to analyze the topological features of the electron density following the topological analysis of the electron density.<sup>17</sup> This analysis allows a description of the contacts and the electronic structure of atoms in molecules. The gradient of the electron density  $\nabla\rho(\mathbf{r}_{CP})$  vanishes at the critical points (CP) corresponding to the extrema of  $\rho(\mathbf{r})$ . The Hessian matrix (tensor of second partial derivatives of  $\rho(\mathbf{r})$ ) generated at the CP points is diagonalized yielding three eigenvalues  $\lambda_1, \lambda_2,$  and  $\lambda_3$ . The eigenvector associated with  $\lambda_3$  is a tangent to the bond path defined as the gradient line connecting the nuclei; those associated with  $\lambda_1$  and  $\lambda_2$  are perpendicular to the bond path. In the case of (3, -1) critical points,  $\lambda_3$  is positive and  $\lambda_1$  and  $\lambda_2$  are negative. Their corresponding sum is the Laplacian of the electron density  $\nabla^2\rho(\mathbf{r}_{CP})$ . Each critical point (CP) is, therefore, characterized by two numbers: the number of different eigenvalues (for non-degenerate cases) and the sum of the signs of the three eigenvalues.

**Electrostatic Potential.** The VMOPRO<sup>11,12</sup> computer program was also used to generate the electrostatic potential based on the Hansen-Coppens electron density model.<sup>10</sup> The electrostatic potential  $\Phi(\mathbf{r})$  at any point  $\mathbf{r}$  around a molecule is calculated as

$$\Phi(\mathbf{r}) = \sum_j \frac{Z_j}{|\mathbf{r} - \mathbf{R}_j|} - \int \frac{\rho_{\text{model},j}(\mathbf{r}')}{|\mathbf{r} - \mathbf{R}_j - \mathbf{r}'|} d\mathbf{r}' \quad (2)$$

where each atom *j* is at position  $\mathbf{R}_j$  in the crystal lattice,  $Z_j$  being its nuclear positive charge. The electrostatic potential determines the nucleophilic (negative potential) and electrophilic (positive potential) regions of the molecule and is an important index of the chemical reactivity.

(17) Bader, R. F. W. *Atoms in Molecules: A Quantum Theory. The International Series of Monographs on Chemistry*, 1st ed.; Oxford: Clarendon Press, 1990; No. 22.

(16) Clementi, E.; Raimondi, D. L. *J. Chem. Phys.* **1963**, *41*, 2686.

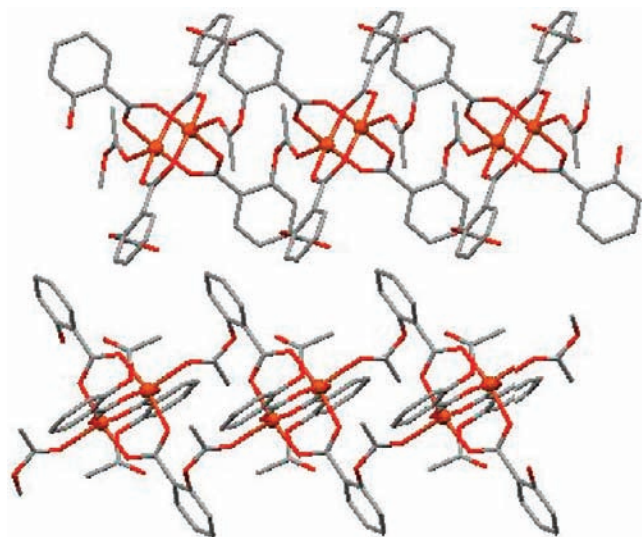


**Figure 2.** Adjacent parallel chains in the crystal structure of the tetrakis- $\mu$ -(acetylsalicylate)dicopper(II) complex. Copper cations are represented as spheres. Hydrogen atoms are omitted for clarity.

## 2. Results and Discussion

**2.1. Crystal Structure.** The crystal structure of the title compound is displayed in Figure 1. The Cu-aspirinate complex crystallizes in the  $P2_1/c$  monoclinic space group.<sup>6,7,9</sup> In the present study, we have refined the structure and electron density in the  $P2_1/n$  space group having a  $\beta$  angle closer to  $90^\circ$  ( $\beta = 98.152(1)^\circ$  instead of  $104.341(8)^\circ$ ).<sup>9</sup> As shown in Figure 1, the copper cation is in a pseudo-octahedral geometry involving five oxygen atoms and one adjacent Cu. Each copper cation is linked to two aspirinate ligands in a bidentate manner. A center of inversion lies between the two adjacent copper atoms with a  $\text{Cu}\cdots\text{Cu}$  link distance of  $2.6054(1)$  Å. This is analogous to the structures reported for dimeric copper benzoylformates where the  $\text{Cu}\cdots\text{Cu}$  distance varies from  $2.725(1)$  to  $2.831(1)$  Å.<sup>18</sup> For comparison, in the copper metal structure the distance is equal to  $2.56$  Å. In the Cu-aspirinate complex, the oxygen atom O4 of the unprimed organic ligand binds a copper cation and plays a role of bridge between  $\text{Cu}_2(\text{Asp})_4$  units. The equivalent O4' (see Figure 1) of the primed aspirinate ligand is, however, not involved in any Cu–O bond. As reported earlier, this original linkage gives rise to a one-dimensional polymeric structure parallel to  $a$ -axis.<sup>9</sup>

The interaction between chains can be considered as van der Waals in nature. Figure 2 displays the adjacent parallel chains observed in the copper-aspirinate crystal, the view is along the  $a$ -crystallographic axis. It is worthy to note that a non-polymeric copper-aspirinate ( $\text{Cu}_2(\text{Asp})_4(\text{DMF})_2$ ) compound has been reported where also a  $\text{Cu}\cdots\text{Cu}$  contact was observed ( $\text{Cu}\cdots\text{Cu} = 2.6154(4)$  Å).<sup>19</sup> This distance is, however, longer than those reported for compounds like  $(\text{CuH})_2$  where the Cu–Cu distance drops to  $2.16$  Å.<sup>20</sup> Table 2 lists the main bond lengths and angles

**Table 2.** Selected Bond Lengths (Å) and Angles (deg) of Tetrakis- $\mu$ -(acetylsalicylate)dicopper(II) Complex<sup>a</sup>

Cu–O2'	1.9646(6)	Cu $\cdots$ Cu <sup>b</sup>	2.6054(1)
Cu–O1'	1.9528(6)	Cu–O4 <sup>c</sup>	2.2183(7)
Cu–O1	1.9598(6)		
Cu–O2 <sup>b</sup>	1.9577(7)		
O1'–Cu–O2'	169.41(3)		
O1–Cu–O2	169.62(3)		
Cu <sup>b</sup> –Cu–O4 <sup>c</sup>	175.90(3)		
O1–C1	1.2652(7)	O1'–C1'	1.2644(7)
O2–C1	1.2615(8)	O2'–C1'	1.2649(7)
O3–C7	1.4020(8)	O3'–C7'	1.3884(8)
O3–C8	1.3514(8)	O3'–C8'	1.3663(9)
O4–C8	1.2149(8)	O4'–C8'	1.2062(10)
C7–C6	1.3846(10)	C7'–C6'	1.3893(10)
C7–C2	1.3966(9)	C7'–C2'	1.4024(9)
C2–C3	1.3982(9)	C2'–C3'	1.4042(9)
C2–C1	1.4954(9)	C2'–C1'	1.4989(9)
C6–C5	1.3963(10)	C6'–C5'	1.3927(11)
C8–C9	1.4919(10)	C8'–C9'	1.4889(13)
C5–C4	1.3950(12)	C5'–C4'	1.3931(11)
C3–C4	1.3935(11)	C3'–C4'	1.3899(10)
O1–C1–C2–C7	–49.0(3)		
O1'–C1'–C2'–C7'	–3.52(7)		
C7–O3–C8–C9	–166.1(7)		
C7'–O3'–C8'–C9'	173.32(7)		

<sup>a</sup> Estimated standard deviations are given in parentheses. <sup>b</sup> Symmetry codes:  $-x, -y-1, -z$ . <sup>c</sup> Symmetry codes:  $-x+1, -y-1, -z$ .

of the title compound. The obtained values are in very good agreement with those reported in the previous study,<sup>9</sup> but the use of low temperature and the refinement of the electron density yield to more accurate bond length and angle estimates. Cu–O distances are on average equal to  $1.96$  Å for the carboxylic oxygen atoms; for the acetyl O4 oxygen, Cu–O4 is longer ( $2.2183(7)$  Å). O–Cu–O angles ( $169.5^\circ$  on average) are equal for oxygen atoms of the two  $\text{COO}^-$  groups of the two aspirinate ligands whereas Cu–Cu–O4 angle is found equal to  $175.90(3)^\circ$ . As reported in Table 2, the C–O and C–C distances are practically equal for the corresponding bonds of the two organic ligands of the asymmetric unit. The main difference lies in the dihedral angles given in Table 2. For the primed aspirinate ligand not involved in the bridging of the  $\text{Cu}_2(\text{Asp})_4$  units, the carboxylate group is almost in the plane of the phenyl ring ( $\text{O1}'\text{–C1}'\text{–C2}'\text{–C7}' = -3.52(7)^\circ$ ) which is not the case for the other ligand ( $\text{O1}\text{–C1}\text{–C2}\text{–C7} = -49.0(3)^\circ$ ). For comparison to our previous study of Zn-aspirinate, the dihedral angle around the corresponding C1–C2 bond was found equal to  $32.32(8)^\circ$ . In Cu-aspirinate, the dihedral angles of the acetyl groups are practically equal for the two ligands ( $-166.1(7)^\circ$  and  $173.32(7)^\circ$ , respectively).

**2.2. Residual and Electron Deformation Densities.** The residual density is calculated and carefully analyzed to judge the quality of the multipole refinement. The residual density is calculated as a Fourier transform of the difference between the observed  $F_o$  and model calculated  $F_c$  structure factors. Figure 3 depicts the residual densities around the copper cation. In these maps, the residual density does not exceed  $0.15 \text{ e } \text{Å}^{-3}$ . Some structured peaks and holes are observed around the copper centers but are too far from the metal sites to be fitted either by the electron density model or by any thermal anharmonicity expansion. Residual density in the rest of the unit

(18) Harada, A.; Tsuchimoto, M.; Ohba, S.; Iwasawa, K.; Tokii, T. *Acta Crystallogr.* **1997**, *B53*, 654.

(19) Viosat, B.; Daran, J. C.; Savouret, G.; Morgant, G.; Greenaway, F. T.; Nguyen-Huy, D.; Pham-Tran, V. A.; Sorenson, J. R. *J. Inorg. Biochem.* **2003**, *96*(2–3), 375.

(20) Koelmel, C.; Ahlrichs, R. *J. Phys. Chem.* **1990**, *94*(14), 5536.

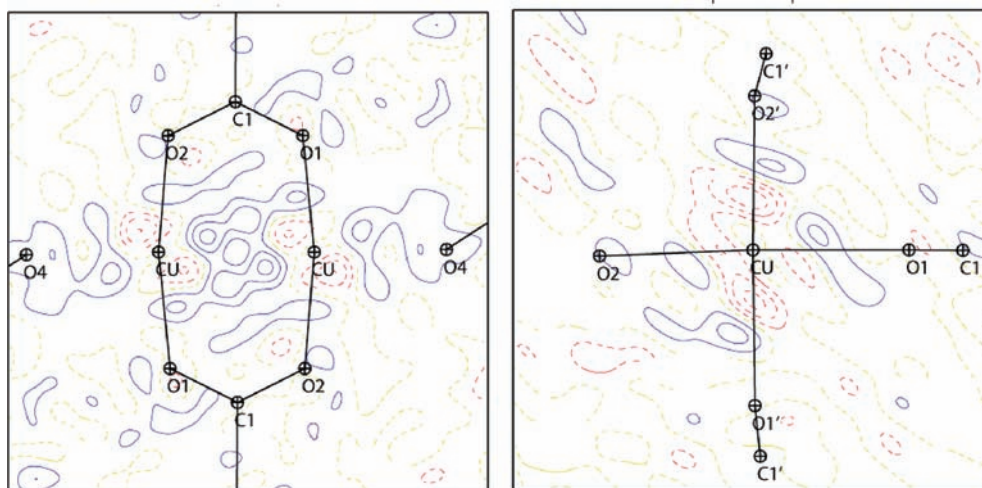


**Figure 3.** Residual density maps around the copper cations. The contour interval is  $0.05 \text{ e } \text{\AA}^{-3}$ , zero and negative contours are dashed. (cutoff of  $(\sin \theta/\lambda) = 0.8 \text{ \AA}^{-1}$ ).

cell is meaningless and not related to any characteristic structural feature, for example, the maximum value (a very sharp peak) equal to  $0.33 \text{ e } \text{\AA}^{-3}$  was found far from all atoms and bonds. Residual density maps in the other planes of the complex are featureless revealing the good fit of the diffraction data with the multipole model.

The static deformation electron density maps are depicted in Figure 4. The static deformation density is calculated in the direct space (no Fourier) using the Hansen–Coppens formula of the electron density. It does not contain any thermal smearing. Generally, it is used like this to be compared to theoretical Hartree-Fock (HF) or density functional theory (DFT) maps. We focus, in this study, on the interaction between the metal and the organic ligands. Continuous contour lines correspond to the accumulation of the electron density and dashed ones correspond to the depletion of the electron density. The copper cations exhibit depleted lobes ( $d_{x^2-y^2}$  orbital) directed toward the carboxylate oxygen atoms O1, O1', O2, and O2' (equatorial plane). This clearly indicates the electrostatic attraction between the metal and the ligand due to the polarized electron density of the oxygen lone pairs (Figure 4). The same features were already discussed by Wang and co-workers in their previous study of the metal square complexes<sup>21</sup> and for a *trans*-bis(cyanamidonitrato-*N*:O)bis-imidazole-*N*<sup>3</sup>)copper(II) compound.<sup>22</sup>

An overall view of the static deformation density is also depicted in Figure 4 for the  $\text{Cu}_2(\text{Asp})_4$  unit using the isodensity surface representation. The deformation density of the copper cations is clearly shown and particularly the depletion of the  $d_{x^2-y^2}$  orbital pointing toward the carboxylate oxygen atoms. What are also shown in this figure are the electron depopulations in the direction of the  $p_z$  orbital of the carbon atoms in carboxylate and phenolic groups as well as the dipolar character of the hydrogen atoms.

### 2.3. Topological Analysis of the Electron Density.

Figure 5 shows the gradient field lines of the electron density in the plane containing the copper cations and the connected carboxylate O1 and O2 oxygen atoms. The atomic basins are defined by the interatomic gradient zero flux surfaces. The  $(3, -1)$  CPs are indicated in Figure 5. The symmetry of the complex shape of the copper cation basin is close to be a cube with nearly planar interatomic surfaces. Oxygen atoms display extended basins whereas those of C1  $sp^2$  carbon atoms are reduced to small trigonal bipyramids. The topological features of the total electron density of the Cu-aspirinate complex are reported in Table 3. The positive sign of the Laplacian  $\nabla^2 \rho(\mathbf{r}_{\text{CP}})$  at the critical points (CPs) for the Cu–O and Cu···Cu contacts shows their closed shell nature. Conversely, all C–C, C–O, C=O, and C–H bonds of the organic ligands exhibit negative Laplacians which are characteristic of shared-shell interactions. The electron concentrations at the CPs for the Cu–O bonds are slightly different ( $0.6$  and  $0.5 \text{ e } \text{\AA}^{-3}$ , respectively) for the carboxylic oxygen atoms of the two aspirinate ligands, even though the Cu–O bond lengths are equal (Table 2). In agreement with the observed distances, both the Laplacian and  $\rho(\mathbf{r}_{\text{CP}})$  of the Cu–O4 bond are smaller in magnitude than those of the other Cu–O bonds. Figure 6 compares the Cu–O1' (short) and Cu–O4 (long) bond features. As the second derivative of the electron density, the negative Laplacian should emphasize the sharp variations of  $\rho(\mathbf{r})$ . It is important to mention that the presence of a bond path is not a necessary condition for a chemical bond.<sup>23–30</sup> So, in this case the presence of a Cu–Cu  $(3, -1)$  CP indicates the presence of a contact. For the Cu···Cu contact (Table 3), the accumulation of

(23) Cioslowski, J.; Mixon, S. T. *J. Am. Chem. Soc.* **1992**, *114*, 4382.

(24) Haaland, A.; Shorokhov, D. J.; Tverdova, N. V. *Chem.—Eur. J.* **2004**, *10*, 4416.

(25) Krapp, A.; Frenking, G. *Chem.—Eur. J.* **2007**, *13*, 8256.

(26) Poater, J.; Visser, R.; Sola, M.; Bickelhaupt, F. M. *J. Org. Chem.* **2007**, *72*, 1134.

(27) Poater, J.; Sola, M.; Bickelhaupt, F. M. *Chem.—Eur. J.* **2006**, *12*, 2902.

(28) Cerpa, E.; Krapp, A.; Vela, A.; Merino, G. *Chem.—Eur. J.* **2008**, *14*, 10232–10234.

(29) Cerpa, E.; Krapp, A.; Flores-Moreno, R.; Donald, K. J.; Merino, G. *Chem.—Eur. J.* **2009**, *15*, 1985–1990.

(30) Bader, R. F. W. *J. Phys. Chem. A* **2009**, *113*, 10391.

(21) Lee, C.-R.; Wang, C.-C.; Chen, K.-C.; Lee, G.-H.; Wang, Y. *J. Phys. Chem. A* **1999**, *103*, 156.

(22) Kozišek, J.; Hansen, N. K.; Fuess, H. *Acta Crystallogr.* **2002**, *B58*, 463.

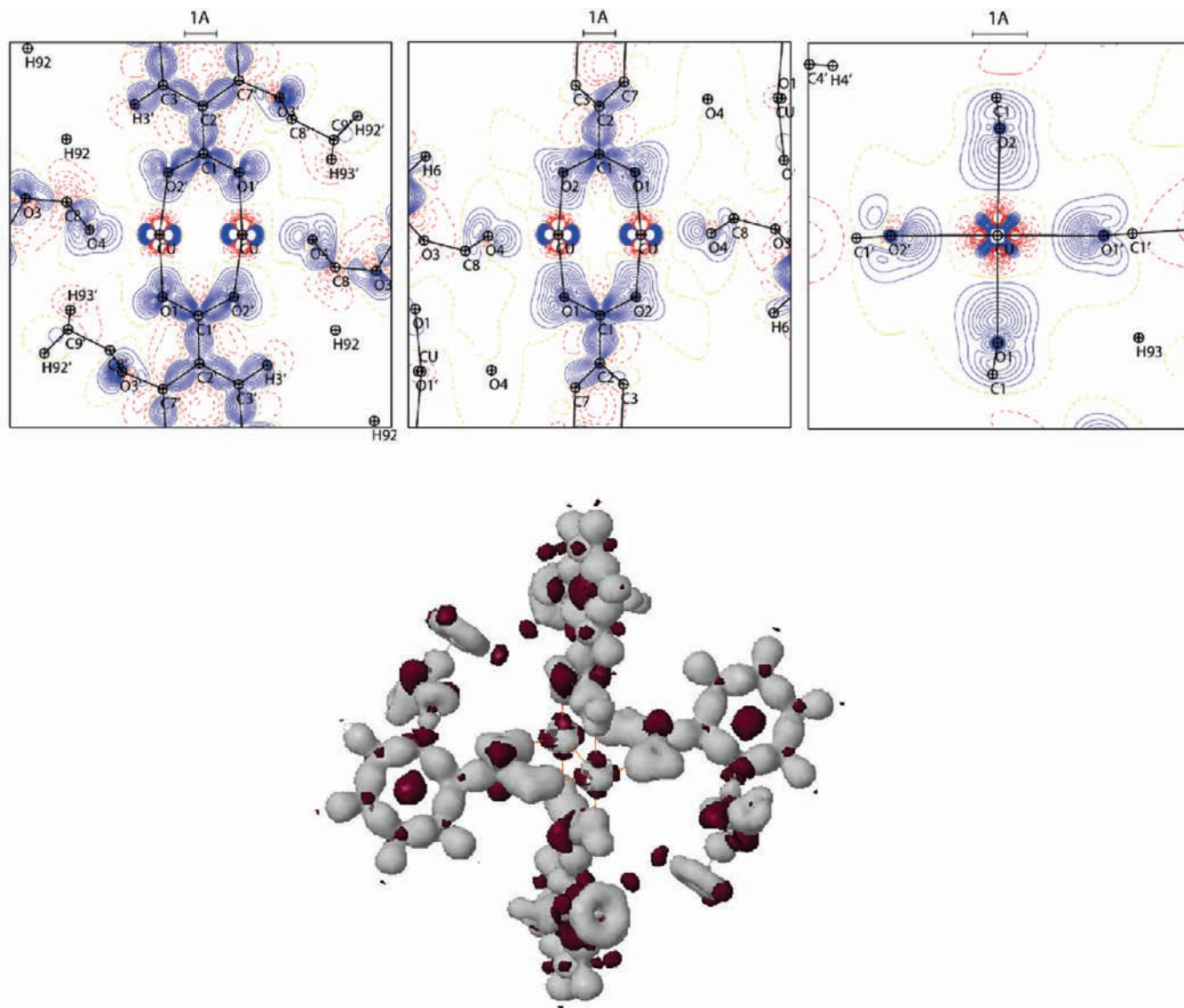


**Figure 4.** Static electron deformation density maps (up) and isosurface representation of the  $\text{Cu}_2(\text{Asp})_4$  unit (down) with the same orientation as in Figure 1. The third electron density map is calculated in the plane of the four oxygen atoms to show the difference of the contraction of the lone pairs. Contour intervals are  $0.05 \text{ e } \text{\AA}^{-3}$ , zero, and negative contours are the dashed lines in the density maps. In isosurface representation, gray and dark isosurfaces correspond to  $\pm 0.14 \text{ e } \text{\AA}^{-3}$ .

the electron density is very small ( $0.09 \text{ e } \text{\AA}^{-3}$ ) associated with a very weak Laplacian ( $1.70 \text{ e } \text{\AA}^{-5}$ ); the standard deviation for  $\rho(\mathbf{r}_{\text{CP}})$  has been previously estimated to be equal to  $0.05 \text{ e } \text{\AA}^{-3}$ .<sup>31</sup> For the ligand parts, topological characteristics are very comparable for primed and unprimed aspirinate anions. The highest magnitudes of both  $\rho(\mathbf{r}_{\text{CP}})$  and  $\nabla^2\rho(\mathbf{r}_{\text{CP}})$  are found for the C–O bonds of the carboxylate groups ( $\rho(\mathbf{r}_{\text{CP}}) \approx 2.8 \text{ e } \text{\AA}^{-3}$  and  $\nabla^2\rho(\mathbf{r}_{\text{CP}})$  values are in the range of  $-30$  to  $-37 \text{ e } \text{\AA}^{-5}$ ). C8=O4 and C8'=O4' double bonds of the acetyl groups exhibit, however, smaller absolute values of Laplacian. The magnitudes of both  $\rho(\mathbf{r}_{\text{CP}})$  and  $\nabla^2\rho(\mathbf{r}_{\text{CP}})$  are lower for the longest C–O bonds involving O3 and O3'. C–C and C–H bonds have topological features comparable to those found in organic molecules.<sup>32</sup> Except for the aromatic

C–H bonds, all C–C of the phenolic rings and methyl C–H exhibit the highest value of the ellipticity  $\epsilon$  on average equal to 0.2 showing delocalized bond.<sup>33</sup>

To quantify the Cu–O bonds and Cu···Cu contact, we have estimated the kinetic, potential, and total energy densities at the CPs using Abramov's approximation:<sup>34</sup>

$$\begin{aligned}
 G(\mathbf{r}) &= \frac{3}{10}(3\pi)^{2/3}\rho^{5/3}(\mathbf{r}) + \frac{1}{6}\nabla^2\rho(\mathbf{r}) \\
 V(\mathbf{r}) &= \frac{1}{4}\nabla^2\rho(\mathbf{r}) - 2G(\mathbf{r}) \\
 E(\mathbf{r}) &= G(\mathbf{r}) + V(\mathbf{r})
 \end{aligned}
 \quad (3)$$

The values are reported in Table 3 in hartree  $\text{\AA}^{-3}$  units. The total energy density is negative for all bonds except

(31) Souhassou, M.; Blessing, R. H. *J. Appl. Crystallogr.* **1999**, *32*, 210.

(32) Benabicha, F.; Pichon-Pesme, V.; Jelsch, C.; Lecomte, C.; Khmou, A. *Acta Crystallogr.* **2000**, *B56*, 155.

(33) Merino, G.; Vela, A.; Heine, T. *Chem. Rev.* **2005**, *105*, 3812–3841.

(34) Abramov, Y. A. *Acta Crystallogr.* **1997**, *A53*, 264.

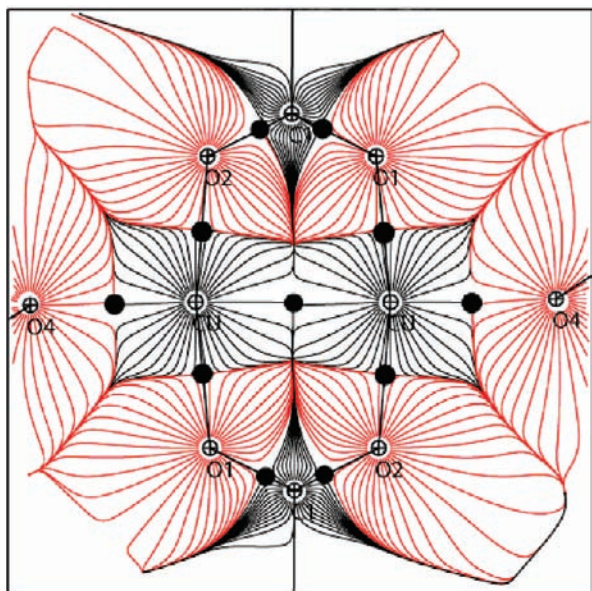


**Figure 5.** Gradient vector field of the electron density of the copper-aspirinate complex. (3, -1) bond critical points are shown as black spheres.

the Cu–O4 and Cu···Cu contacts. These calculations clearly demonstrate that the largest interaction of the copper cation is obtained with the unprimed ligand ( $-0.12$  hartree  $\text{\AA}^{-3}$ ) compared to primed ligand ( $-0.03$  hartree  $\text{\AA}^{-3}$ ). Even though the total energy density  $E(\mathbf{r}_{\text{CP}})$  is negative, the ratio  $G(\mathbf{r}_{\text{CP}})/\rho(\mathbf{r}_{\text{CP}})$  is, however, greater than unity for all these bonds indicating their ionic character.<sup>34</sup> For the Cu–O4 and Cu···Cu contacts, the total energy density is positive and  $G(\mathbf{r}_{\text{CP}})/\rho(\mathbf{r}_{\text{CP}})$  is greater to unity emphasizing a slight ionic character for this bond compared to the other Cu–O ones. For the Cu···Cu contact, no information can be drawn for this contact and the nature of the bond from the topological analysis. In a recent electron density study of 3-amino-propanolato Cu(II) complexes,<sup>35</sup> the Cu cation is in a square-planar configuration with short two Cu–O (1.93  $\text{\AA}$  on average) and one Cu–N (1.98  $\text{\AA}$  on average) bonds. Another oxygen atom of an adjacent complex is connected to the copper cation but at a longer distance (2.5 to 2.7  $\text{\AA}$ ). The values reported for the Cu–O bond energy densities are in good agreement with those of the present study. However, the total energy density found equal to  $-0.12$  hartree  $\text{\AA}^{-3}$  for Cu–O1 and Cu–O2 in copper-aspirinate is higher than those reported for the short Cu–O distance in the 3-amino-propanolato Cu(II) complexes; only the Cu–N bonds in the latter compound exhibit comparable values of  $E(\mathbf{r}_{\text{CP}})$  emphasizing the known nitrophilic property of copper.

#### 2.4. Atomic Charges and d-Orbital Populations of Cu.

The multipole parameters have been used to estimate the copper 3d orbital populations.<sup>36</sup> We recall that the  $z$ -axis chosen for the copper cation local frame is directed along the Cu···Cu contact (or Cu–O4 elongated bond, 2.2183(7)  $\text{\AA}$ ) and the  $x$ -axis is toward O1. The obtained values are listed in Table 4. They are in agreement with

the features shown in the deformation density maps (Figure 4). The  $d_{z^2}$  population is slightly greater than 2.0 which is often observed when a small overlap of charge density occurs like here for Cu with O4 atom and when the bond has a covalent character.<sup>37</sup> A normalization of the absolute 3d population for Cu to 2e will give a 2e population for  $d_{z^2}$ , 1.611e for  $d_{xy}$  and  $d_{yz}$ , 1.579 for  $d_{xy}$  and 1.022 for  $d_{x^2-y^2}$ . The charge transfer from the  $d_{x^2-y^2}$  may also increase the  $d_{z^2}$  population. Populations of  $d_{xy}$ ,  $d_{xz}$ , and  $d_{yz}$  are practically equal. The most depopulated orbital (1.17 e instead of 2.0) is the  $d_{x^2-y^2}$  one with lobes pointing toward the carboxylic oxygen atoms. These results show that the electronic configuration of Cu in the copper-aspirinate complex is close to  $[\text{Ar}]3d^94s^0$ . This is in agreement with the electronic configuration of  $\text{Cu}^{2+}$  used for example in the refinement of  $(\text{ND}_4)_2\text{Cu}(\text{SO}_4) \cdot 2.6\text{D}_2\text{O}$ .<sup>38,39</sup> Unfortunately, in our investigation no information on the 4s (the most diffuse orbital) population can be provided.

The  $\kappa$ -refinement was carried out to assign the atomic charges.<sup>40</sup> The results are given in Table 5. The valence population obtained for the copper cation corresponds to a charge of +1.20(3) e. This value is very comparable to that reported for the Zn-aspirinate complex with a Zn charge of +1.29(4) e.<sup>5</sup> O1, O2, and O1', O2' oxygen atoms bonded to Cu have net charge magnitudes ranging from  $-0.52$  (O1') to  $-0.77$  e (O1). C1 and C1' carbon atoms of the carboxylic groups carry +0.48(6) and +0.63(6) e, respectively. This last value is very comparable to the charge obtained for the corresponding C1 carbon atom in Zn-aspirinate (+0.60(6) e).<sup>5</sup> In Cu-aspirinate, O3 and O3' have the same charge of  $-0.30(4)$  e whereas those of the ester oxygen atoms O4 and O4' are  $-0.67(4)$  and  $-0.44(5)$  e, respectively. It is worthy to note that such a difference is to be expected since O4 is bonded to Cu but not O4'. The connected carbon atoms C8 and C8' also exhibit different charges of +0.72(6) and +0.59(7) e, respectively. The corresponding charge obtained in Zn-aspirinate was +0.8 e showing that the electrophilic character of this acetyl carbon is slightly weaker in the Cu-aspirinate compound. As reported earlier,<sup>5</sup> the biological activity of aspirin involves the carbon C8 in the acetylation of the aminoacids of the COX-2 cyclooxygenase.<sup>41</sup> The less positive charges of C8 and C8' in Cu-aspirinate are compensated by high values of the C9 and C9' charges found equal to  $-0.92(10)$  and  $-1.29(12)$  e, respectively; a charge of  $-0.79$  e was found for C9 in the Zn-aspirinate complex. This also gives rise to high charge values of the methyl hydrogen atoms (+0.34 and +0.48 e in unprimed and primed ligands) compared to +0.17 e found in the Zn-aspirinate complex. This trend holds true for the aromatic hydrogen atoms;  $\kappa$  parameters for H atoms are, however, higher for the title compound.

(37) Pillet, S.; Souhassou, M.; Mathonière, C.; Lecomte, C. *J. Am. Chem. Soc.* **2004**, *126*, 1219.

(38) Figgis, B. N.; Khor, L.; Kucharski, E. S.; Reynolds, P. A. *Acta Crystallogr.* **1992**, *B48*, 144.

(39) Figgis, B. N.; Iversen, B. B.; Larsen, F. K.; Reynolds, P. A. *Acta Crystallogr.* **1993**, *B49*, 794.

(40) Coppens, P.; Guru Row, T. N.; Leung, P.; Stevens, E. D.; Becker, P. J.; Yang, Y. W. *Acta Crystallogr.* **1979**, *A35*, 63.

(41) Hochgesang, G. P., Jr.; Rowlinson, S. W.; Marnett, L. J. *J. Am. Chem. Soc.* **2000**, *122*, 6514.

(35) Farrugia, L. J.; Middlemiss, D. S.; Sillanpää, R.; Seppälä, P. *J. Phys. Chem. A* **2008**, *112*, 9050.

(36) Holladay, A.; Leung, P.; Coppens, P. *Acta Crystallogr.* **1983**, *A39*, 377.

**Table 3.** Topological Properties of the Tetrakis- $\mu$ -(acetylsalicylate)dicopper(II) Complex<sup>a</sup>

	$d_1$	$d_2$	$\rho(r_{\text{CP}})$	$\nabla^2\rho(r_{\text{CP}})$	$\lambda_1$	$\lambda_2$	$\lambda_3$	$\varepsilon$	$G(r_{\text{CP}})$	$V(r_{\text{CP}})$	$E(r_{\text{CP}})$
Cu O1	0.967	0.993	0.61	10.82	-3.43	-3.42	17.67	0.00	0.86	-0.95	-0.11
Cu O2	0.969	0.989	0.63	10.30	-3.50	-3.46	17.26	0.01	0.85	-0.98	-0.13
Cu O1'	0.973	0.980	0.55	11.47	-3.19	-3.12	17.79	0.02	0.83	-0.86	-0.03
Cu O2'	0.979	0.986	0.52	11.05	-3.01	-2.99	17.05	0.01	0.78	-0.80	-0.02
Cu O4	1.089	1.130	0.28	5.20	-1.41	-1.35	7.96	0.04	0.33	-0.31	0.02
Cu Cu	1.303	1.303	0.09	1.70	-0.29	-0.28	2.27	0.04	0.09	-0.07	0.02
O1 C1	0.788	0.477	2.74	-35.25	-24.36	-22.53	11.64	0.08			
O2 C1	0.799	0.462	2.80	-37.19	-25.30	-23.90	12.01	0.06			
O4 C8	0.806	0.408	2.91	-15.13	-29.03	-25.43	39.33	0.12			
O3 C7	0.835	0.567	1.83	-11.57	-13.31	-13.16	14.91	0.01			
O3 C8	0.854	0.498	2.09	-22.77	-16.13	-15.94	9.30	0.01			
C2 C1	0.726	0.770	1.85	-13.89	-13.24	-12.24	11.59	0.08			
C2 C3	0.708	0.691	2.13	-17.80	-15.53	-13.04	10.76	0.16			
C7 C2	0.704	0.694	2.19	-19.06	-16.82	-13.35	11.11	0.21			
C7 C6	0.708	0.676	2.22	-20.81	-16.84	-13.84	9.87	0.18			
C3 C4	0.688	0.706	2.19	-19.78	-16.10	-13.62	9.94	0.15			
C5 C4	0.697	0.699	2.19	-20.01	-16.56	-13.90	10.44	0.16			
C6 C5	0.685	0.711	2.14	-18.99	-15.88	-13.46	10.35	0.15			
C8 C9	0.823	0.668	1.76	-14.15	-11.89	-10.82	8.56	0.09			
C3 H3	0.731	0.352	1.77	-17.14	-16.61	-15.76	15.23	0.05			
C9 H91	0.705	0.355	1.60	-12.98	-14.87	-11.94	13.83	0.20			
O1' C1'	0.766	0.498	2.76	-34.68	-25.82	-23.23	14.36	0.10			
O2' C1'	0.815	0.449	2.64	-29.93	-25.30	-23.06	18.42	0.09			
O4' C8'	0.803	0.406	2.92	-13.44	-29.40	-25.81	41.77	0.12			
O3' C7'	0.837	0.552	1.83	-13.24	-14.36	-13.02	14.14	0.09			
O3' C8'	0.848	0.519	2.05	-21.08	-15.43	-15.42	9.78	0.00			
C2' C1'	0.719	0.780	1.76	-12.37	-13.10	-10.97	11.71	0.16			
C2' C3'	0.694	0.710	2.07	-17.77	-15.27	-12.91	10.40	0.15			
C7' C2'	0.712	0.690	2.12	-19.09	-16.64	-12.91	10.45	0.22			
C7' C6'	0.698	0.693	2.15	-19.80	-16.48	-13.40	10.07	0.19			
C3' C4'	0.682	0.708	2.17	-19.78	-16.23	-13.70	10.14	0.16			
C5' C4''	0.697	0.697	2.19	-20.15	-16.61	-13.94	10.40	0.16			
C6' C5'	0.682	0.710	2.15	-19.33	-16.02	-13.55	10.24	0.15			
C8' C9'	0.821	0.670	1.75	-14.20	-11.91	-10.85	8.55	0.09			
C3' H3'	0.728	0.355	1.74	-16.83	-16.51	-15.62	15.30	0.05			
C9' H91'	0.701	0.359	1.58	-12.79	-14.66	-11.68	13.54	0.20			

<sup>a</sup>  $\rho(r_{\text{CP}})$  and  $\nabla^2\rho(r_{\text{CP}})$  are the electron density and the Laplacian values at the critical points (CP) with the three eigenvalues  $\lambda_1$ ,  $\lambda_2$ , and  $\lambda_3$ ;  $\varepsilon$  is the ellipticity and  $d_1$  and  $d_2$  designate the corresponding atom-CP distances.  $G(r_{\text{CP}})$ ,  $V(r_{\text{CP}})$ , and  $E(r_{\text{CP}})$  are the kinetic, potential, and total energy densities (in Hartree  $\text{\AA}^{-3}$  unit), respectively.

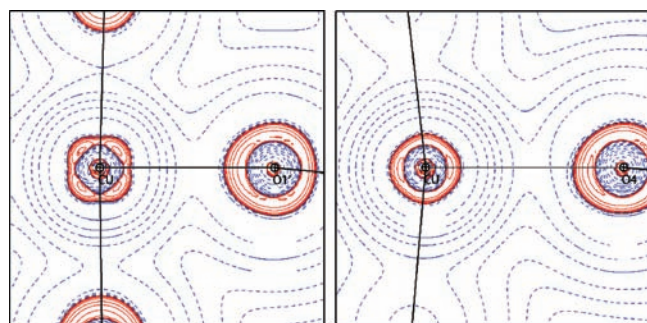


**Figure 6.** Contour map of negative Laplacian  $-\nabla^2\rho(r)$  comparing the features of Cu-O1' and Cu-O4 bonds. Solid contours denote concentrations of electronic charge; negative contours are in the regions of charge depletion. Contour levels are at  $2.10^n$ ,  $4.10^n$ , and  $8.10^n$  ( $n = -3, -2, -1, 0, 1, 2, 3$ )  $e \text{\AA}^{-5}$ .

**2.5. Electrostatic Potential.** The atomic multipole parameters were also used to generate the electrostatic

**Table 4.** 3d Atomic Orbital Populations (in e unit) for Cu in the Tetrakis- $\mu$ -(acetylsalicylate)dicopper(II) Complex

$d_{z^2}$	$d_{xz}$	$d_{yz}$	$d_{x^2-y^2}$	$d_{xy}$	sum
2.290	1.845	1.845	1.170	1.808	8.958

potential (eq 2). The electrostatic potential maps are displayed in Figure 7. The chosen planes are the same as for the electron density (Figure 4). All surrounding  $\text{Cu}_2(\text{Asp})_4$  unit contributions are accounted for in this calculation. In our previous study of Zn-aspirinate, however, a  $\text{Zn}(\text{Asp})_2$  unit can be isolated from the crystal lattice. In contrast to the reported highly positive electrostatic potential for *trans*-bis(cyanamidonitrato-*N*:O)bisimidazole-*N*<sup>3</sup>copper(II) complex,<sup>22</sup> the positive contribution of the copper cations in Cu-aspirinate are attenuated by the negative electrostatic potential of the ligands. The deepest electrostatic potential is found in the vicinity of O1 and O2 oxygen atoms and reaches  $-0.2 e \text{\AA}^{-1}$ .



In the plane containing the primed ligand ( $O1'-Cu-O2'$ ), the regions of negative electrostatic potential are reduced

**Table 5.**  $\kappa$  Parameters and Valence Populations ( $P_{val}$ ) of the Tetrakis- $\mu$ -(acetylsalicylate)dycopper(II) Complex after the  $\kappa$ -Refinement<sup>a</sup>

	$\kappa$	$P_{val}$		$\kappa$	$P_{val}$
Cu	1.034(3)	8.80(3)			
O1	0.971(4)	6.77(5)	O1'	0.988(4)	6.52(4)
O2	0.984(4)	6.58(4)	O2'	0.984(4)	6.56(4)
O3	0.997(4)	6.29(4)	O3'	0.989(4)	6.30(4)
O4	0.977(4)	6.67(4)	O4'	0.966(4)	6.44(5)
C1	1.088(9)	3.52(6)	C1'	1.104(10)	3.37(6)
C2	1.033(7)	4.40(6)	C2'	1.045(8)	4.17(6)
C3=C4=C5=C6	1.026(4)	4.32(3)	C3'	1.059(4)	3.99(3)
C7	1.060(8)	3.84(6)	C7'	1.072(9)	3.73(6)
C8	1.092(10)	3.28(6)	C8'	1.073(11)	3.41(7)
C9	0.980(9)	4.92(10)	C9'	0.942(9)	5.29(12)
H3=H4=H5=H6	1.289(27)	0.78(2)	H3'	1.271(27)	0.82(3)
H91=H92=H93	1.328(49)	0.66(4)	H91'	1.284(61)	0.52(4)

<sup>a</sup> Estimated standard deviations are given in parentheses.

because of the positive contribution of the in-plane phenolic ring.

These features are shown well in the isosurface representation of the electrostatic potential of an isolated  $Cu_2(Asp)_4$  unit also depicted in Figure 7. An extended negative electrostatic potential surface envelops the phenolic rings of the unprimed aspirinate ligands whereas primed ligands display a positive electrostatic potential (electrophilic character). The negative surface is pierced in the vicinity of the copper cations. This window of a positive electrostatic potential corresponds to the attraction site of the adjacent O4 oxygen atom of a second ligand in the  $Cu_2(Asp)_4$  unit chain. The same trends are observed for the isopotential surfaces generated by the  $\kappa$ -refinement parameters (Table 5). Both positive and negative regions are, however, more extended. The unprimed aspirinate ligands are now totally covered by the negative electrostatic potential surface. These characteristics are expectable from the determined charges of the two organic ligands. Indeed, from the values given in Table 5, the total charges of unprimed and primed ligands are equal to  $-1.6$  and  $+0.4$  e, respectively.

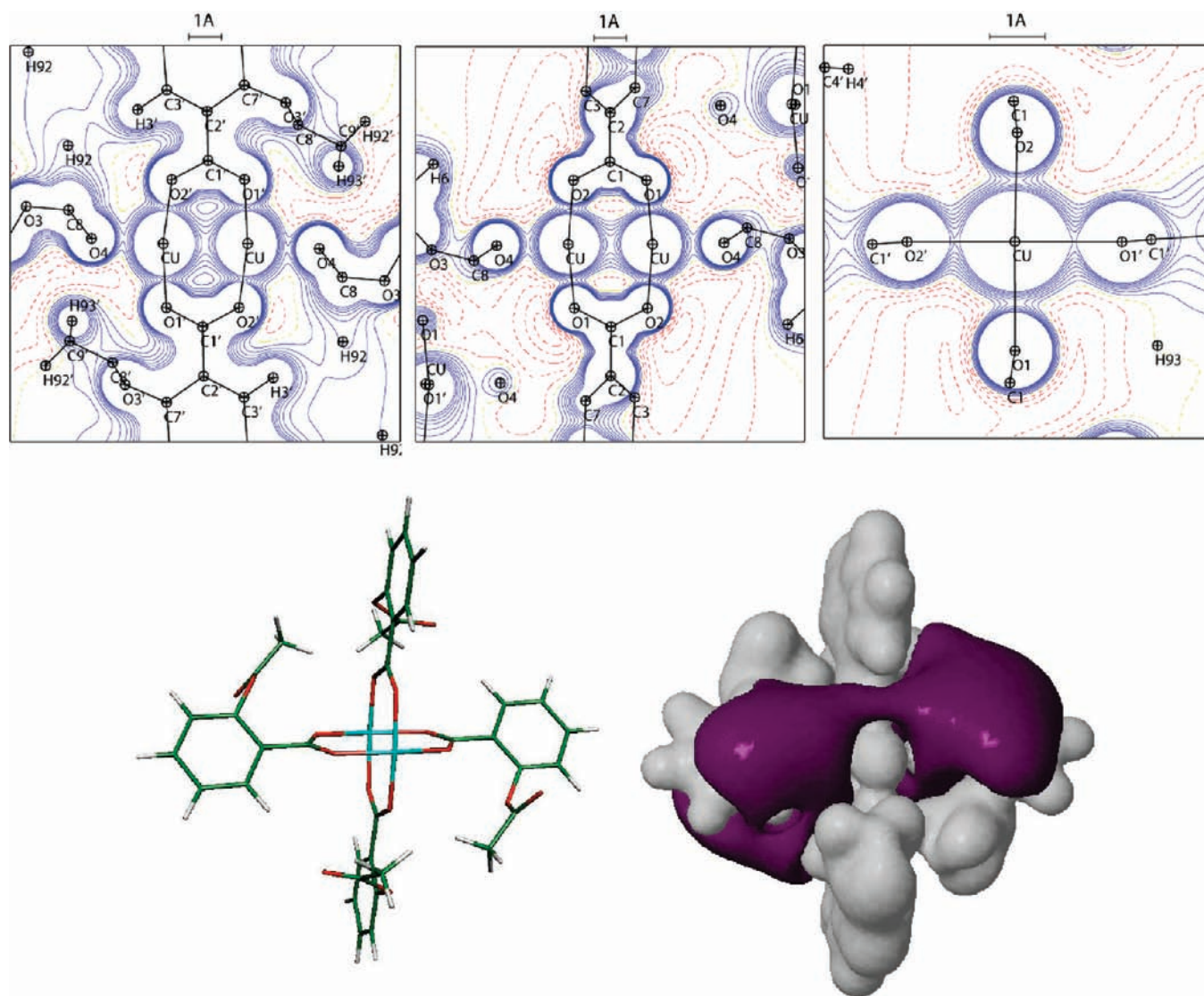


**Figure 7.** Electrostatic potential maps (up) and isopotential surfaces of the  $Cu_2(Asp)_4$  unit (down). Contour intervals are  $0.05 \text{ e } \text{\AA}^{-1}$ , zero and negative contours are dashed lines in the electrostatic potential maps. In the isosurface representation, gray and dark isodensities correspond to  $\pm 0.10 \text{ e } \text{\AA}^{-1}$ . The electrostatic potential was generated by all multipole populations.

The anionicity of the unprimed ligand connected to two copper cations through O1, O2 on one hand and O4 on the other hand, is naturally strengthened. For comparison, in the  $\text{Zn}(\text{Asp})_2(\text{H}_2\text{O})_2$  complex unit, a charge of  $-0.65$  e was reported for the aspirinate anion.

### 3. Conclusions

The experimental electron density study of copper-aspirinate clearly reveals the metal–ligand interaction. Features of the electron deformation density and electrostatic potential are presented. The topology of the electron density quantifies the characteristics of the atomic bonds of the organic part, the Cu–O bonds, and the Cu···Cu contact, as well. The atomic charges are reported revealing a  $3d^94s^1$  configuration of Cu in the title compound. The deformation electron density and the 3d population analysis show that the most depopulated (1.17 e) orbital is the  $d_{x^2-y^2}$  one, that

pointing toward the carboxylic oxygen atoms of the aspirinate ligands. Finally, the electrophilic character of the acetyl carbon, responsible of the activity of the aspirin drug, remains in the copper-aspirinate complex, accounting for its biological activity.

**Acknowledgment.** The financial support of the CNRS, Ecole Centrale Paris, Université de Paris Sud 11, Université Cadi Ayyad, Universidad de las Américas-Puebla and Benemérita Universidad Autónoma de Puebla is gratefully acknowledged. M.M.R. is thankful to CONACYT (Fondo Mixto Puebla No. 9019) for financial support. The authors are grateful to the reviewers for their insightful comments and suggestions.

**Supporting Information Available:** Atomic coordinates and multipole parameters. This material is available free of charge via the Internet at <http://pubs.acs.org>.